

Direct spectroscopic observation of the atomic-scale mechanisms of clustering and homogenization of rare-earth dopant ions in vitreous silica

Sabyasachi Sen

Department of Chemical Engineering & Materials Science, UC Davis, California 95616, USA

Rafail Rakhmatullin and Ruslan Gubaidullin

MRS Laboratory, Kazan State University, Kremlevskay 18, 420008 Kazan, Russia

Andreas Pöpl

Faculty of Physics and Earth Sciences, University of Leipzig, Linnéstr. 5, D-04103 Leipzig, Germany

(Received 10 July 2006; published 27 September 2006)

Structural aspects of clustering of rare earth ions in oxide glasses have been studied for the last several years in relation to their applications in photonics. However, the mechanism of homogenization of the spatial distribution of rare earth ions by codoping, typically with Al or P, is still not well understood. In this work we report direct experimental determination of the homogenization mechanism of Yb^{3+} ion clusters in silica glasses doped with 0.1 wt. % Yb_2O_3 and codoped with Al or P, using two-dimensional HYSORE-EPR spectroscopy. The results lead us to conclude that Yb creates its coordination environment via formation of Yb-O-Si and Yb-O-Yb bonds in a Yb-doped silica glass and even the light codoping with Al starts replacing these bonds with Yb-O-Al linkages. Heavy codoping with P replaces all Yb-O-Si/Yb linkages with Yb-O-P linkages. The formation of a next-nearest neighbor shell of Al or P creates suitable structural pockets, which ultimately leads to homogenization.

DOI: [10.1103/PhysRevB.74.100201](https://doi.org/10.1103/PhysRevB.74.100201)

PACS number(s): 61.43.Fs, 76.30.Kg, 76.30.-v

Glasses doped with rare-earth (RE) ions (e.g., Nd^{3+} , Er^{3+} , Tm^{3+} , Yb^{3+}) have found important technological applications in recent years as solid-state lasers and more importantly as optical fiber amplifiers for all-optical telecommunication networks.¹ High levels of RE doping (several wt. %) are required in glasses for their potential applications in photonics, for fabricating miniature optical devices such as microchip lasers and lossless splitters.²⁻⁵ However, due to their low solubility in SiO_2 -rich silicate glasses, the dopant RE ions tend to cluster even at doping levels of a few hundred to a few thousand parts per million (ppm) by weight.⁶⁻⁸ Such clustering of RE ions gives rise to cross relaxation between excited ion pairs within a cluster that results in nonradiative deexcitation of the ion pair. The resultant concentration quenching of fluorescence drastically lowers the quantum efficiency of compact photonic devices.¹ Our understanding of the intermediate-range structural aspects of RE clustering in glasses including cluster size and intra-cluster RE-RE distances have remained largely rudimentary in spite of the extensive structural studies of these materials using a variety of spectroscopic techniques in the recent past.^{1,4,6-12} In terms of local coordination environment of the rare earth ions clustering may correspond to the formation of R-O-R type of linkages ($R=\text{RE}$) in the glass structure. Previous spectroscopic studies of Nd-doped SiO_2 and Yb-doped GeO_2 glasses have shown strong evidence in favor of the formation of Nd-O-Nd and Yb-O-Yb linkages in the glass structure, at doping levels of only a few hundred to a few thousands of ppm by weight of Nd_2O_3 or Yb_2O_3 .⁸⁻¹⁰ It has also been shown that codoping these glasses with a second high field strength ion such as Al or P results in a breakup of these clusters and a partial to complete homogenization in the spatial distribution of the RE ions.^{6,8-10} However, the structural

length scales associated with the clustering process and the atomic-scale mechanism of the homogenization process are still not well understood.

Recent developments in two-dimensional (2D) pulsed electron paramagnetic resonance (EPR) spectroscopic techniques have enabled researchers to obtain structural information beyond the nearest-neighbor coordination environments of paramagnetic centers present at low concentrations in glasses.⁹ We report here the results of the application of 2D hyperfine sublevel correlation (HYSORE) EPR spectroscopy to obtain a direct atomic-scale understanding of the homogenization process of dopant Yb^{3+} ions in vitreous SiO_2 glass on codoping with Al and P. Yb has been chosen as a model RE ion since Yb-doped glasses have shown significant potential in recent years as candidates for high-power fiber laser and amplifier applications in the 1 μm wavelength region.^{13,14}

The SiO_2 glasses used in this study were doped with 0.1 wt. % (1000 ppm) Yb_2O_3 and were codoped with either Al such that the Al:Yb atomic ratio is $\sim 3:1$ or with P such that the P:Yb atomic ratio is $\sim 10:1$. All glass samples were prepared by conventional melt quenching method. The Yb-Al-codoped glass sample was prepared from high-purity constituent oxides. In the case of synthesis of the Yb-P-codoped SiO_2 glass, an Yb-doped SiO_2 glass, and a binary 30% P_2O_5 -70% SiO_2 glass were used as batch materials. The Yb- SiO_2 glass was prepared by melting a mixture of constituent oxides while phosphoric acid was used as the source of P for the synthesis of the 30% P_2O_5 -70% SiO_2 glass. The batch materials were finely crushed in an agate mortar, contained in 80% Pt-20% Rh crucibles and were melted at 1800 °C for 3 h in a furnace (Deltech DT-33-CVT-912) in air. These melts were cooled in

air and the resulting glasses were finely crushed and remelted for another 3 h at 1800 °C to ensure chemical homogeneity and finally quenched in water.

All EPR measurements were carried out using a pulsed EPR spectrometer (Bruker ESP 380) in the X band at 5 K. The echo detected EPR (EDEPR) spectra of different samples were collected using two-pulse echo sequences: $\pi/2$ - τ - π - τ -echo or $2\pi/3$ - τ - $2\pi/3$ - τ -echo while sweeping the magnetic field. For EDEPR typical π -pulse length of 24 ns, $\pi/2$ -pulse length of 16 ns, $2\pi/3$ -pulse length of 96 ns and time delays τ ranging from 200 to 600 ns were used.

The HYSORE spectroscopy is a two-dimensional extension of the familiar three pulse electron spin echo envelope modulation (ESEEM) technique with an additional mixing π -pulse which improves the resolution and provides information that is not easily obtained from one-dimensional ESEEM spectra. It has been used successfully especially in disordered systems to study the hyperfine interactions (HFI) between electron spins and nearby nuclei with nonzero nuclear spin I .^{9,15,16} The interpretation of the HYSORE spectra is often simpler than that of the one-dimensional ESEEM spectra especially in the case of hyperfine coupling with quadrupolar nuclei with $I > 1/2$ that results in overlapping nuclear transition frequencies.¹⁵⁻¹⁷ The pulse sequence $\pi/2$ - τ - $\pi/2$ - t_1 - π - t_2 - $\pi/2$ - τ -echo is typically used for HYSORE measurements. The first two $\pi/2$ pulses create the nuclear coherence between the sublevels of the electron-nuclear spin manifolds. The populations of these manifolds are exchanged by the π pulse after the evolution period t_1 . The resulting correlation between the corresponding nuclear transitions is detected with a $\pi/2$ pulse after a time t_2 in the form of an echo.¹⁷ A π -pulse length of 16 ns and a $\pi/2$ -pulse length of 24 ns were used in our HYSORE experiments. A four-step phase cycle was applied in order to avoid interferences of unwanted echoes.¹⁷ Starting values of t_1 and t_2 in the pulse sequence were 96 ns. The time increment in both dimensions was chosen to be 16 ns at various τ values.

The echo detected EPR (EDEPR) spectra for the glass sample of SiO₂ doped with Yb³⁺ and codoped with P₂O₅ (hereafter SYP) and for the sample of SiO₂ doped with Yb³⁺ and codoped with Al₂O₃ (hereafter SYA) are shown in Fig. 1. An echo signal was observed at zero magnetic field only for the SYA sample. It should be noted that Yb³⁺ is a Kramers ion with $S=1/2$ and has no zero field splitting.¹⁸ Theoretically the g value for Yb³⁺ cannot exceed $2\Lambda * M$, where M is the maximum value of the projection of the full angular momentum, and Λ is the Lande factor for Yb³⁺. The main term for Yb³⁺ is ${}^2F_{7/2}$, which yields values for $\Lambda=8/7$ and hence for $g_{\max} \approx 8$, indicating that for our working frequency of ~ 9.73 GHz no EPR absorption should be observable at magnetic fields below ~ 80 mT for uncoupled Yb³⁺ ions. This statement is valid for even isotopes of Yb (Yb¹⁶⁸, Yb¹⁷⁰, Yb¹⁷², Yb¹⁷⁴, and Yb¹⁷⁶) that have 69.6% of the total natural abundance.¹⁹ Besides there are odd isotopes, Yb¹⁷¹ with nuclear spin $I=1/2$ and Yb¹⁷³ with $I=5/2$ having 14.28% and 16.13% of the natural abundance, respectively. Intensities of the hyperfine lines are approximately an order of magnitude weaker for Yb¹⁷¹ and even more for Yb¹⁷³ in comparison with the Zeeman lines of the even isotopes. The typical overall spread of the hyperfine splitting is approxi-

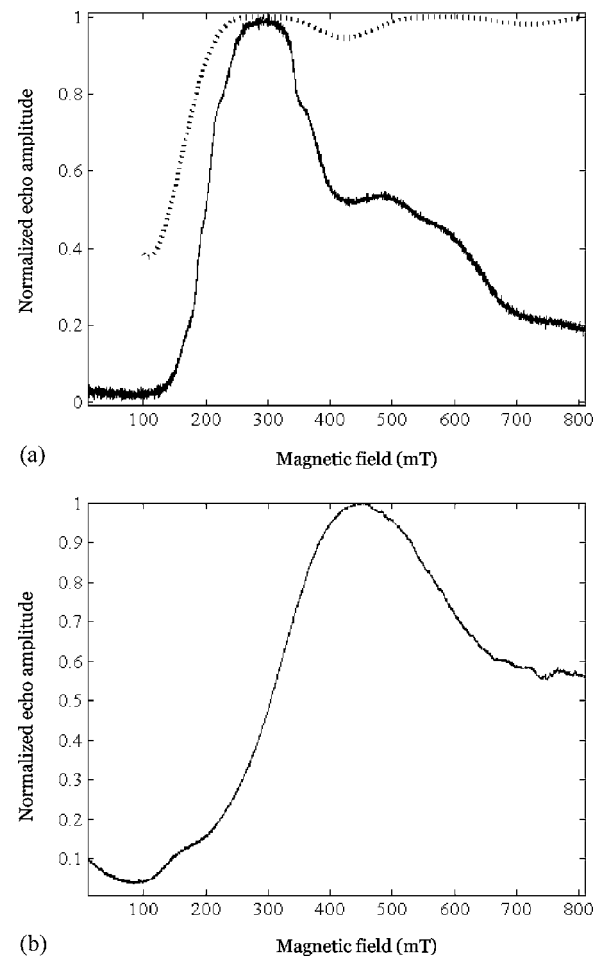


FIG. 1. Field-swept Yb³⁺ EDEPR spectra of (a) SYP and (b) SYA glasses. Both spectra were collected with a two-pulse echo sequence $\pi/2$ - τ - π - τ -echo with $\pi/2$ pulse length=16 ns, π pulse length=24 ns, and $\tau=200$ ns. The broken line in (a) is the magnetic field dependence of echo amplitude, calculated for hyperfine coupling with neighboring ³¹P nuclei and $\tau=200$ ns (see text for details).

mately 60 mT for the odd isotopes of Yb³⁺. Hence, for uncoupled Yb³⁺ ions no EPR signal should be observed corresponding to any Yb³⁺ isotope for the working frequency of 9.73 GHz at zero field. In that case the only reasonable explanation for the observation of an echo at lower fields in the case of SYA sample is the formation of pairs or more complex clusters of Yb³⁺ ions. Previous EDEPR studies of Yb-doped GeO₂ glasses and cw-EPR line shape simulations have indicated that such clustering of Yb³⁺ ions corresponds to the formation of Yb-O-Yb linkages in the glass structure.⁸ The presence of Yb³⁺ ion clusters in the SYA glass points toward the fact that the relatively low level of Al codoping with Al:Yb atomic ratio of $\sim 3:1$ is not sufficient to break up the Yb-O-Yb linkages. On the other hand the lack of any evidence of clustering in the SYP glass is consistent with the high level of P codoping in this glass with P:Yb atomic ratio of $\sim 10:1$. These results are also consistent with previous fluorescence line-narrowing studies of Al/P and RE codoped SiO₂ glasses, which have indicated that complete homogenization of RE dopants requires high Al/P codoping levels

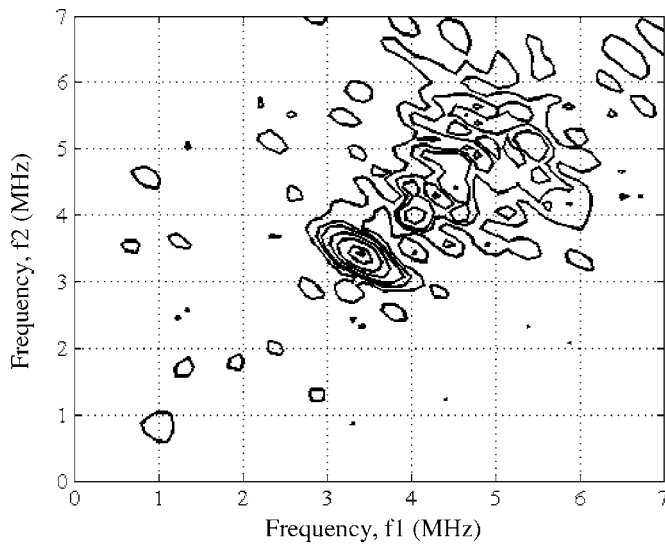


FIG. 2. Contour plot of 2D-HYSCORE spectrum of the SYA glass sample recorded at a magnetic field of 400 mT with a π pulse length=16 ns, $\pi/2$ pulse length=24 ns, and $\tau=136$ ns (see text for other details).

such that Al/P:RE atomic ratio is $\sim 10:1$ or higher.⁶ The Yb^{3+} EDEPR spectrum of the SYP glass shows modulation arising from hyperfine coupling with nuclei that have non-zero nuclear spin (Fig. 1). The broken line in Fig. 1(a) is the magnetic field dependence of echo modulation amplitude V , calculated for ^{31}P nuclei and $\tau=200$ ns according to the approximate relation²⁰

$$\langle V(B, \tau) \rangle = 1 - \frac{3T_{\perp}^2}{10\nu_i^2} [3 - 4 \cos(2\pi\nu_i\tau) + \cos 2\pi(2\nu_i\tau)], \quad (1)$$

where T_{\perp} is the perpendicular element of the anisotropic HFI tensor with eigenvalues $(T_{\perp}, T_{\perp}, -2T_{\perp})$, ν_i is the nuclear Larmor frequency, τ is time delay between microwave pulses. The field dependence results from the dependence of $\nu_i = g\beta B/h$, where B is the magnetic field value and β is the Bohr magneton. Equation (1) was solved for $V(B, \tau)$ with the approximations of a weak anisotropic HFI and an isotropic g -tensor. A comparison between the calculated $V(B, \tau)$ and the experimental Yb^{3+} EDEPR spectrum of the SYP glass indicates that the latter is consistent with the presence of ^{31}P nuclei in the vicinity of the Yb^{3+} ions in this glass (Fig. 1). It should be noted here that the Yb^{3+} EDEPR spectrum of the SYA sample may also be influenced by the neighboring ^{27}Al nuclei. However, fast damping of echo oscillations resulting from the large quadrupole moment of the ^{27}Al nuclei may preclude the experimental observation of such oscillations.

The HYSCORE spectra for the SYA and SYP glasses, collected at 400 and 348 mT, respectively, are shown in Figs. 2 and 3, respectively. These spectra show peaks only along the diagonal. The most pronounced peak in the HYSCORE spectrum of the SYA sample can readily be assigned to neighboring Si atoms as the frequency of this peak corresponds well with the Larmor frequency of ^{29}Si nuclei which

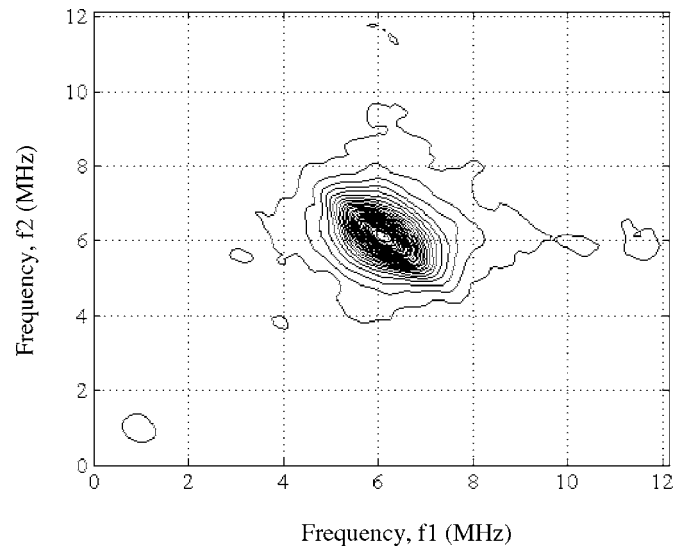


FIG. 3. Contour plot of 2D-HYSCORE spectrum of the SYP glass sample recorded at a magnetic field of 348 mT, with a π pulse length=16 ns, $\pi/2$ pulse length=24 ns, and $\tau=104$ ns (see text for other details).

is ~ 3.38 MHz at 400 mT (Fig. 2). This result implies that there is a weak anisotropic ligand HFI of Yb^{3+} ions with neighboring Si^{29} nuclei. The direct observation of Si neighbors is an interesting result by itself considering the fact that the natural abundance of the ^{29}Si isotope is only 4.67%. Assuming the isotropic ligand HFI $a_{iso}=0$, an approximate estimation of the distance between Yb^{3+} ion and a ^{29}Si nucleus can be made within the dipolar point approximation using the formula for the perpendicular element T_{\perp} of anisotropic HFI tensor¹⁷

$$T_{\perp} = \frac{\mu_0 g_e g_n \beta_e \beta_n}{4\pi\hbar R^3}, \quad (2)$$

where, μ_0 is permeability of vacuum, g_e , g_n are electron and nuclear g values and β_e and β_n are Bohr and nuclear magnetons, respectively. T_{\perp} in our case is equivalent to the electron-nucleus dipolar coupling constant. T_{\perp} can be estimated from the maximum frequency shift $\Delta\nu_{\max}$ from the antidiagonal in the HYSCORE spectrum at nuclear Larmor frequency ν_i using the following relation²¹:

$$\Delta\nu_{\max} = \sqrt{2} \frac{9}{32} \frac{T_{\perp}^2}{\nu_i}. \quad (3)$$

However, $\Delta\nu_{\max}$ in the HYSCORE spectrum of the SYA glass was found to be too small such that Eq. (3) could not be used reliably for an approximate estimation of the average Yb-Si distance. Instead T_{\perp} was roughly estimated from the extension of the ridges for $a_{iso}=0$, with the assumption that all orientation of the powder spectrum are present. Equation (2), with this rough estimation of the T_{\perp} yields an average Yb-Si distance of ~ 4.2 Å in the SYA glass. Such Yb-Si distances are consistent with the presence of Yb-O-Si linkages in the glass structure. Besides the strong ^{29}Si peak, the HYSCORE spectrum of the SYA glass also shows a weak signal at ~ 4.44 MHz that can be assigned to the Larmor

frequency of ^{27}Al nuclei at 400 mT (Fig. 2). Unfortunately, the ^{27}Al signal is too weak to reliably estimate the Yb-Al distances in this glass. However, similar spectral signature from ^{27}Al nuclei has been observed in a previous study, in the HYSORE spectra of Nd and Al codoped SiO_2 glasses where the Nd-Al distance was estimated to be 3.5 Å indicating formation of Nd-O-Al linkages in the glass structure.⁹ Thus, the HYSORE spectrum of the SYA glass provides direct evidence in favor of the formation of Yb-O-Al linkages in the structure, even at such low doping levels of Al. The codoping of the Yb-doped SiO_2 glass with Al_2O_3 therefore immediately results in replacement of the next-nearest neighbors in the second coordination shell of Yb^{3+} ions. Such a change in the intermediate-range environment must play a key role in homogenization of the spatial distribution of Yb. This hypothesis is corroborated by the HYSORE spectrum of the SYP glass which shows a single strong peak at ~ 6.0 MHz that corresponds to the Larmor frequency of ^{31}P at 348 mT (Fig. 3). Calculations on the basis of Eqs. (2) and (3) yield an average Yb-P distance of ~ 4.0 Å in the SYP glass. The complete lack of any peak in the HYSORE spectrum corresponding to ^{29}Si nuclei as well as the absence of any echo signal at zero magnetic field for the SYP glass indicate a complete replacement of the Yb-O-Si and Yb-O-Yb linkages with Yb-O-P linkages. It may be noted here that the phase relaxation times for the Yb^{3+} ions are found to be extremely short in these glasses (~ 250 ns), which may preclude direct observation of Yb next-nearest

neighbors in the HYSORE spectrum. This is because the relaxation times of Yb-Yb pairs/clusters may be too short, at the fields used for the HYSORE experiments reported here, to observe electron spin echoes or modulations on the weak echo from pairs/clusters.

Hence, a consistent and detailed structural picture of homogenization of the RE clusters in SiO_2 glass emerges when the EDEPR and HYSORE results for the SYA and SYP glasses are taken together. The introduction of Yb_2O_3 in SiO_2 glass at a doping level of ~ 1000 ppm results in clustering and the second coordination shell of Yb^{3+} ions consists of both Yb and Si resulting in the formation of Yb-O-Yb and Yb-O-Si linkages. These Yb and Si next-nearest neighbors start getting replaced by Al or P even at low levels of codoping (Al/P:Yb atomic ratio of $\sim 3:1$) and such replacement becomes complete as the level of codoping increases such that Al/P:Yb atomic ratio is $\sim 10:1$. Thus codoping with Al or P results in the formation of structural pockets in the glass consisting of Yb^{3+} ions with oxygen nearest neighbors and Al/P next-nearest neighbors. Such structural pockets give rise to homogenization of RE clusters via a spatial redistribution of the Yb^{3+} ions in the glass structure and an increase in the average Yb-Yb separation distance in the SiO_2 glass structure.

R.M.R. is grateful to DAAD for funding to carry out the EPR measurements at the Leipzig University.

¹Rare Earth Doped Fiber Lasers and Amplifiers, edited by M. J. F. Digonnet (Marcel Dekker, New York, 2001).

²K. Hattori, T. Kitagawa, M. Oguma, M. Wada, J. Temmyo, and M. Horiguchi, *Electron. Lett.* **29**, 357 (1993).

³J. J. Zayhowski, *Opt. Mater.* **11**, 255 (1999).

⁴A. I. Smirnov and S. Sen, *J. Chem. Phys.* **115**, 7650 (2001).

⁵I. M. Thomas, J. D. Payne, and G. D. Wilke, *J. Non-Cryst. Solids* **151**, 183 (1993).

⁶K. Arai, H. Namikawa, K. Kumata, T. Honda, Y. Ishii, and T. Handa, *J. Appl. Phys.* **59**, 3430 (1986).

⁷P. Goldner, B. Schaudel, and M. Prassas, *Phys. Rev. B* **65**, 054103 (2002).

⁸S. Sen, R. Rakhmatullin, R. Gubaydullin, and A. Silakov, *J. Non-Cryst. Solids* **333**, 22 (2004).

⁹S. Sen, S. B. Orlinskii, and R. M. Rakhmatullin, *J. Appl. Phys.* **89**, 2308 (2001).

¹⁰S. Sen, *J. Non-Cryst. Solids* **261**, 226 (2000).

¹¹F. Auzel and P. Goldner, *Opt. Mater.* **16**, 93 (2001).

¹²A. Monteil, S. Chaussedent, G. Alombert-Goget, N. Gaumer, J. Obriot, S. J. L. Ribeiro, Y. Messaddeq, A. Chiasera, and M. Ferrari, *J. Non-Cryst. Solids* **348**, 44 (2004).

¹³M. J. Dejneka, B. Z. Hanson, S. G. Crigler, L. A. Zenteno, J. D. Minelly, D. C. Allan, W. J. Miller, and D. Kuksenkov, *J. Am. Ceram. Soc.* **85**, 1100 (2002).

¹⁴R. Paschotta, J. Nilsson, A. C. Trooper, and D. C. Hanna, *IEEE J. Quantum Electron.* **QE-33**, 1049 (1997).

¹⁵G. Kordas, *Phys. Rev. B* **68**, 024202 (2003).

¹⁶L. Astrakas, Y. Deligiannakis, G. Mitrikas, and G. Kordas, *J. Chem. Phys.* **109**, 8612 (1998).

¹⁷A. Schweiger and G. Jeschke, *Principles of Pulse Electron Paramagnetic Resonance* (Oxford University Press, New York, 2001).

¹⁸A. Abragam and B. Bleaney, *Electron Paramagnetic Resonance of Transition Ions* (Clarendon Press, Oxford, 1970).

¹⁹B. M. Kozyrev and S. A. Al'tshuler, *Electron Paramagnetic Resonance in Compounds of Transition Elements* (Wiley, New York, 1974).

²⁰S. A. Dikanov and Yu. D. Tsvetkov, *Electron Spin Echo Envelope Modulation (ESEEM) Spectroscopy* (CRC Press, Boca Raton, 1992).

²¹A. Pöpl and L. Kevan, *J. Chem. Phys.* **100**, 3387 (1996).